

# Mechanical and Superconducting Properties of Multifilamentary Nb<sub>3</sub>Sn Composites

By

Kozo OSAMURA, Shojiro OCHIAI and Toshihiro UEHARA

(Received March 30, 1989)

## Abstract

The interrelation of mechanical and superconducting properties with the microstructure of multifilamentary composites has been investigated. The fracture behaviour changed depending on the growth of the compound layer. When the layer is thin, multiple fracture is observed and the composite can be plastically deformed with a large elongation. On the other hand, when the heat treatment progresses and the layer thickness becomes thicker, the whole composite fractures at once after a small elastic elongation. There exists a critical thickness dividing these two modes, which has been determined theoretically as well as experimentally. The maximum global pinning force can be well described as a function of the inverse grain size of the compound. The strength of the compound is also made clear so as to be expressed as a function of the inverse grain size. Finally, we propose the structure of composites and the conditions of heat treatment to optimize both properties mentioned above.

## 1. Introduction

Nb<sub>3</sub>Sn is recognized as one of the most promising superconducting materials for high field application. This compound, however, is brittle and fractures at low strain, which results in a limited strain tolerance for the design of superconductors 1). Therefore, it is very important to know their deformation and fracture behaviour as well as their influence on superconducting properties. Till now, much effort has been directed towards clarifying the prestrain effects on superconducting characteristics. The deformation and fracture behaviour itself have been scarcely investigated. In our recent works 2), 3), 4), the room temperature tensile behaviour of the compound layer in bronze-processed multifilamentary superconducting composites has been investigated, changing the microstructures mainly by heat treatment. It was found that the strength of compounds decreases with an increasing grain size. Although the strain to fracture of the compound layer is very low, the whole composite can give high elongation in a condition, at which the drop of the load bearing capacity due to breakage of the compound

\* Department of Metallurgy, Kyoto University, Sakyo-ku, Kyoto 606, Japan

could be compensated by strain hardening of ductile constituents. To get an optimized condition for performance, it is required to make clear the quantitative relation of the mechanical properties with its microstructures. In the present work, we have investigated both the mechanical and superconducting properties of the multifilamentary composites. Through the analysis of the microstructure dependence of these properties, it has been suggested that both the tensile properties and the superconducting critical current can be predicted in terms of the condition of heat treatment.

## 2. Experimental Procedure

The specimens used here were the multifilamentary composites supplied as the Japanese Standard Reference Sample for the research group of superconducting materials for the energy research in 1983—1985 of the Ministry of Education, Science and Culture of Japan. The composite specimens were composed of 745 Nb filaments in Cu-7.4at%Sn bronze, surrounded with an Nb barrier and then pure copper as a stabilizer. The bronze ratio and the copper to non-copper one were 2 and 0.445, respectively. Two types of specimens with different diameters were mainly used as listed in Table 1.

Table 1 Dimensions of multifilamentary composites investigated here.

Specimen	$d_c/\text{mm}$	$d_f/\mu\text{m}$	$c_b/\mu\text{m}$
S1	0.311	5.3	7.1
S2	2.6	44.7	59.3

$d_c$ : diameter of the specimen,  
 $d_f$ : diameter of Nb filament,  
 $c_b$ : thickness of Nb barrier

The details of heat treatments employed here are listed in Table 2. The thickness of the compound layer,  $c$ , the diameter of the Nb filament,  $d_f - 2c$ , the distance between filaments,  $L_f$  and the Sn concentration of the bronze matrix,  $x_{\text{Sn}}$ , were measured by means of SEM and EPMA from the polished cross-section of the specimen. From the fracture surface, the grain size of  $\text{Nb}_3\text{Sn}$ ,  $d$ , was determined with the linear-line-intercept method. A tensile test was performed with an Instron type tensile machine at room temperature at a strain rate of  $3.33 \times 10^{-3} \text{s}^{-1}$ . The critical current,  $I_c$ , was measured in the range of the magnetic field from 2 to 8 T, partially up to 15 T at 4.2 K with  $1 \mu\text{V}/\text{cm}$  criterion. The critical current density,  $J_c^0$ , is defined as  $J_c^0 = I_c / S_{\text{Nb}_3\text{Sn}}$ , where  $S_{\text{Nb}_3\text{Sn}}$  is the total cross-sectional area of compound layers in the composite. Then the global pinning force,  $F_p^0 (= J_c^0 \times B)$  was obtained.

Table 2 Condition of heat treatment

Type	T <sub>A</sub> /K	t <sub>A</sub> /ks	Specimen
HT1	873	1.7	S1
	1073	4320	S2
HT2#	1123	86.4	S1
	1273		

# : after preannealing at 973 K for 432 ks.

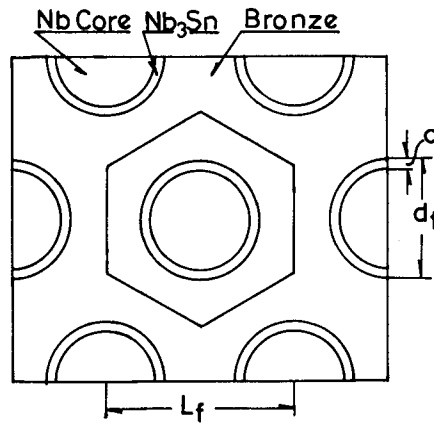


Fig. 1 Schematic representation of the cross section of a multifilamentary composite.

### 3. Experimental Results and Discussion

By using the experimental data reported recently 2), 3), the general feature of the microstructure in the multifilamentary composite was discussed as follows. The bronze ratio, B<sub>r</sub>, is defined as shown in Fig. 1. The composite consists of identical hexagons, of which the center is occupied by the Nb filament. The ratio without the compound layer is given by the equation,

$$B_r = 2\sqrt{3} (L_f/d_f)^2/\pi - 1. \tag{1}$$

During the formation of the compound Nb<sub>3</sub>Sn layer, Sn atoms in each hexagon diffuse inside and react with the Nb filament. In order to produce the compound layer with a thickness of c, the decrease of the Sn concentration in the matrix can be expressed as

$$\Delta x_{\text{Sn}} = \frac{v_b c}{B_r v_c d_f} \left(1 - \frac{c}{d_f}\right), \quad (2)$$

where  $v_b$  and  $v_c$  are the average atomic volumes of the bronze and the compound, respectively. Fig. 2 shows the relation between the Sn concentration of bronze and the reduced thickness of the compound layer,  $c/d_f$ . By fitting Eq. (2) with the data, the parameter  $v_b/v_c$  was found to become 0.76, which is consistent with the estimated value of 0.67 from the lattice parameter at room temperature. When the equilibrium Sn concentration with the compound is assumed to be nearly zero, the maximum thickness of the compound formed,  $(c/d_f)_\infty$ , was estimated to be 0.276.

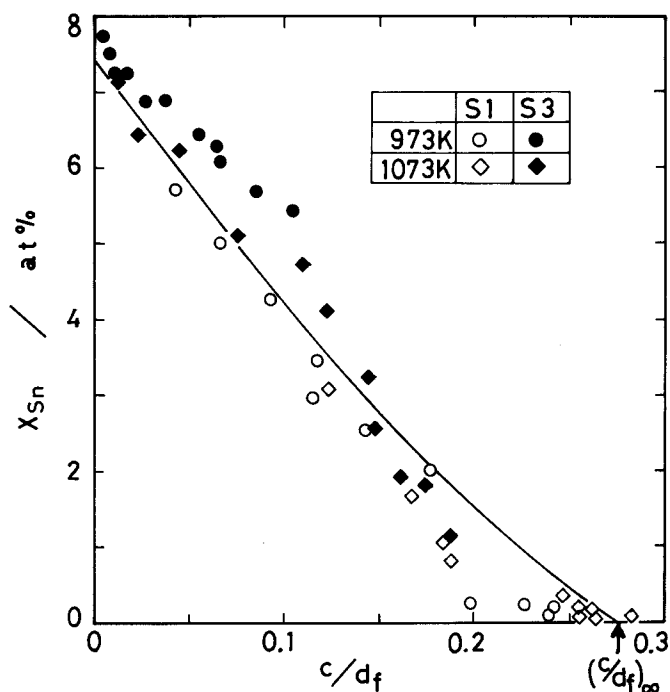


Fig. 2 Relation between the Sn concentration in the bronze matrix and the thickness of compound layer.

The increasing rate of layer thickness becomes slow down in the multifilamentary composite after a long time annealing, because of the depletion of the Sn concentration in the bronze matrix. This behaviour can be understood by solving the diffusion equation. Here one dimensional model has been considered. Supposing a system with the length of  $2L$  as the bronze matrix. The initial condition is  $x_{\text{Sn}} = x_{\text{Sn}}^0$  for  $-L < \zeta < L$  at  $t = 0$ , and the boundary condition for  $t > 0$  is  $x_{\text{Sn}} = x_{\text{Sn}}^1$  at  $\zeta = -L$  and  $\zeta = L$  and  $dx_{\text{Sn}}/d\zeta = 0$  at  $\zeta = 0$ . At  $t > 0$ , the solute atoms flow out through the boundaries. When  $m_t$  denotes the

total amount of diffusing substance which has flowed out from the system at time t, and m<sub>∞</sub> the corresponding quantity after infinite time, then the ratio is given by the equation 5),

$$M(\tau) = \frac{m_t}{m_\infty} = 1 - \sum_{N=0}^{\infty} \frac{8}{(2N+1)^2 \pi^2} \exp\left[-\frac{\pi^2}{4}(2N+1)^2 \tau^2\right], \tag{3}$$

where  $\tau$  is given by  $\sqrt{(Dt)}/L$ . As the whole amount of Sn atoms diffused out from the system react with Nb to form the compound, the following proportionality holds,

$$c/d_f = (c/d_f)_\infty M(\tau). \tag{4}$$

Here the maximum value of  $(c/d_f)_\infty$  is 0.276 as shown in Fig. 2 and substituted in Eq. (4). The numerical evaluation of Eq. (4) is displayed by the solid curve in Fig. 3. The experimental data have been adjusted with its theoretical curve by assuming the next diffusion constant,

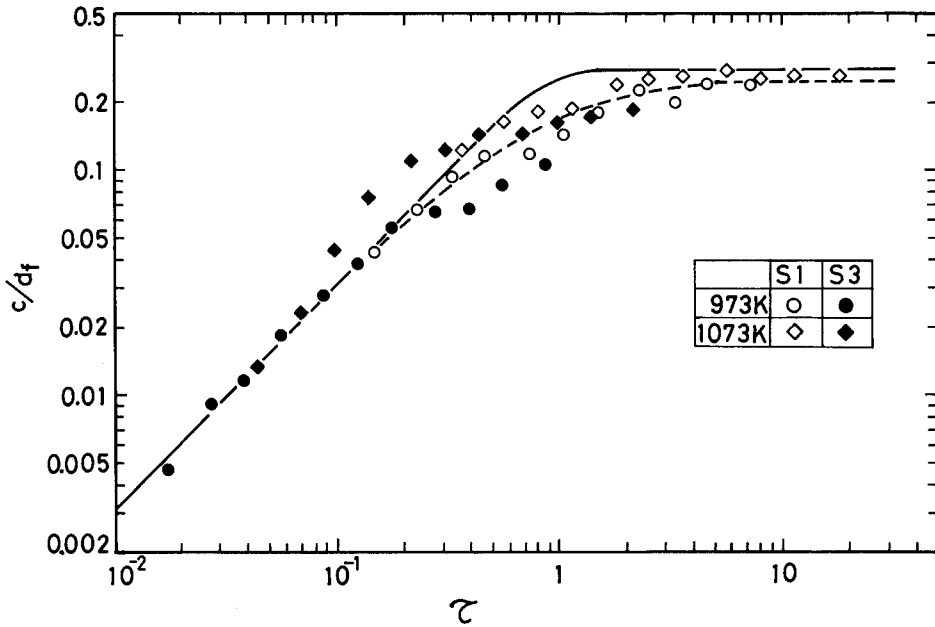


Fig. 3 Change of reduced thickness of the compound layer as a function of characteristic time.

$$D = 9.1 \times 10^{-9} \exp(-156000/RT), \tag{5}$$

where the activation energy was used as the same for the interdiffusivity in the bronze 6). It is clear that the experimental data are well scaled with each other and consistent with the theoretical curve in the small region of  $\tau$ . The inconsistency between the experiments and the theory might be explained by two aspects. As the diffusivity depends

on the Sn concentration  $\delta$ ), the flow rate of the Sn atoms decreases with annealing time, and then the growth rate of the compound layer retards. To explain exactly the experimental data, two dimensional diffusion equations should be solved instead of the present one-dimensional model. At present, the fitting function is empirically proposed as

$$c/d_f = 0.25(1 - \exp(-1.24\tau)), \quad (6)$$

which is displayed by the dotted curve in Fig. 3.

It is observed that the grain of  $\text{Nb}_3\text{Sn}$  grows either during the isothermal annealing or during the isochronal one. To express these time and temperature dependences of grain growth, we could deduce the following fitting function in the unit of  $\mu\text{m}$ ,

$$d = 96 \times t^{0.1} \exp(-59500/RT). \quad (7)$$

A comparison of Eq. (7) with the experimental data is shown in Fig. 4. Thus, Eq. (7) is found to be satisfactorily used in the wide range of the annealing condition.

There are two distinct behaviours for the fracture mode of the composite, temporarily called type I and II<sup>2,3</sup>). In type I, the apparent plastic deformation of the composite as a whole is observed and the elongation to fracture  $e_c$  is high. The compound layer shows a multiple fracture. In type II, such an apparent plastic deformation is not

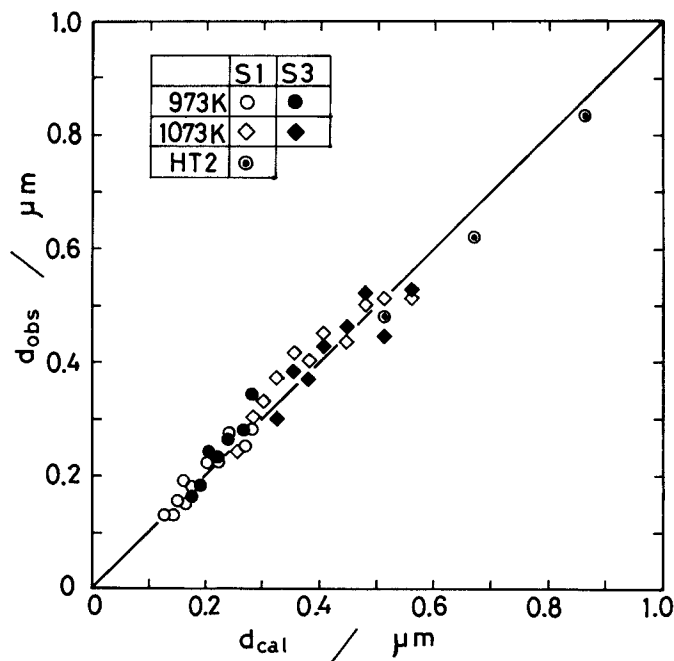


Fig. 4 Comparison of grain sizes of  $\text{Nb}_3\text{Sn}$  observed from the fracture surface and calculated from Eq. (7).

found and the  $e_c$  is low, usually less than 1%. The specimens fracture in a brittle manner. The compound layer does not show any multiple fracture. The type I mode occurs when the composite is annealed for a shorter time at a higher temperature, but otherwise type II occurs, especially for long time annealing. The elongation,  $e_c$ , is a good measure to distinguish the fracture mode. Fig. 5 shows the dependence of the elongation as a function of  $c/d_f$ . The type I mode occurs when  $c/d_f$  is less than about 0.2. Here, the solid curve is the theoretical result as mentioned later. The vertical line shows the limit of the type I mode for each specimen with a different filament diameter and heat treatment. The elongation for type I keeps a high value and drops abruptly by a transition of the fracture mode to type II.

In the type I mode, the drop of the load bearing capacity of the composite as a whole due to the breakage of the compound can be compensated by work hardening of the ductile constituents of Cu, Cu-Sn and Nb. The stress can be transferred to the once-fractured compound layer, which again fractures into shorter lengths. On the other hand, in type II, the fracture of the compound layer causes a fracture of the composite as a whole. This fracture mode is described as the noncumulative mode, which occurs when a few of the compound layers break, followed by a chain reaction of the fracture of the remaining compound layers. The transition of the fracture mode from type I to type II is understood as follows. According to the rule of mixtures, the stress of the composite at the fracture of the compound layer,  $\sigma_c^A$ , is given by

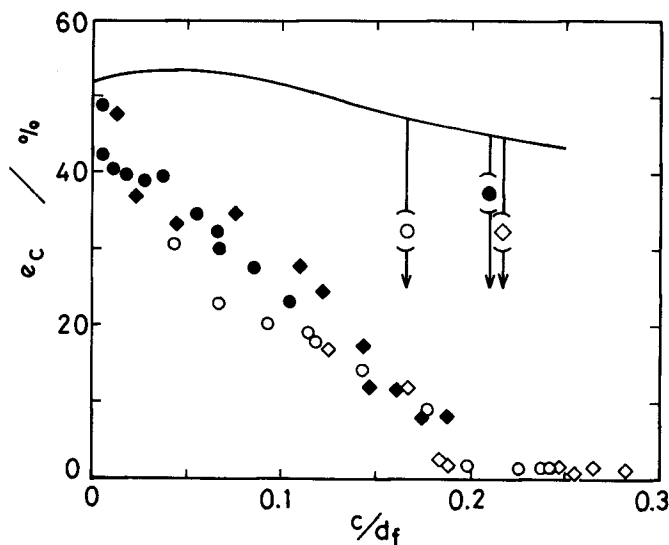


Fig. 5 Change of elongation to fracture as a function of the reduced layer thickness, where the solid curve is the theoretical result.

$$\sigma_c^A = \sigma_{\text{Nb}_3\text{Sn}} V_{\text{Nb}_3\text{Sn}} + \sigma_{\text{Cu}}^\dagger V_{\text{Cu}} + \sigma_{\text{Cu-Sn}}^\dagger V_{\text{Cu-Sn}} + \sigma_{\text{Nb}}^\dagger V_{\text{Nb}} \quad (8)$$

where  $\sigma_i$  and  $V_i$  are the stress and volume fractions of the constituent. The  $\sigma_c^A$  is consistent with the yield stress of the composite. As the elongation is relatively small, say less than 1 %, each value of  $\sigma_c^\dagger$  will be the same as the yield stress for each constituent. Thus, the fracture stress of  $\text{Nb}_3\text{Sn}$  is estimated from the above equation, because all other quantities are obtainable by the experiments. The result is shown in Fig. 6. The stress is well expressed as a function of the grain size of  $\text{Nb}_3$  in the unit of MPa,

$$\sigma_{\text{Nb}_3\text{Sn}} = 560d^{-0.68} \quad (9)$$

Here the exponent is nearly equal to  $-0.5$  indicating that the fracture stress is described by the Hall-Petch relation (4).

The strength of the composite showing a large plastic deformation with a multiple fracture of the compound layer,  $\sigma_c^B$ , can be expressed as

$$\sigma_c^B = \sigma_{\text{duc}} V_{\text{duc}} + \sigma'_{\text{Nb}_3\text{Sn}} V_{\text{Nb}_3\text{Sn}}, \quad (10)$$

where  $\sigma_{\text{duc}}$  the stress capacity of the ductile constituents,  $V_{\text{duc}}$  is the sum of the volume fractions of Cu, Cu-Sn and Nb, and  $\sigma'_{\text{Nb}_3\text{Sn}}$  is the contribution of the compound layer after the multiple fracture. When the elongation due to plastic deformation is large, the contribution to the stress from work hardening is taken into consideration. At the nor-

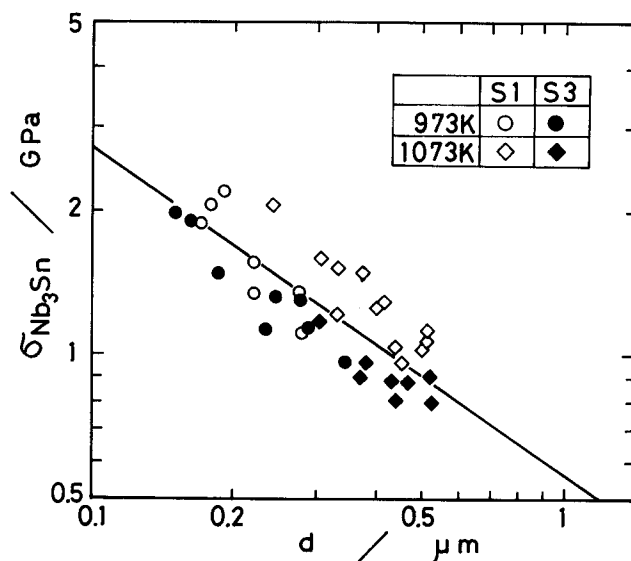


Fig. 6 Grain size dependence of the strength of compound layer.



mal elongation,  $e$ , the normal stress is given by

$$\sigma_{duc} = \sum_i (a_i + b_i \varepsilon)^{n_i} V_i \exp(-\varepsilon) / V_{duc}, \tag{11}$$

where  $i = \text{Cu, Cu-Sn and Nb}$  and  $\varepsilon$  is the true plastic strain given as  $\varepsilon = \ln(1 + e)$ . The maximum stress capacity of the ductile constituents as a whole is determined from the condition at  $e = e_{max}$ ,

$$d\sigma_{duc}/de = 0. \tag{12}$$

The stress supported by the segmented compound layer,  $\sigma'_{\text{Nb}_3\text{Sn}}$  3), was neglected in the present discussion because its contribution is relatively small. Thus  $\sigma_c^B$  can be evaluated through the above mentioned procedure. In practice,  $\sigma_c^B > \sigma_c^A$ , then the composite can be plastically deformed. The maximum elongation is given by  $e_{max}$  from Eq. (12), and the ultimate tensile strength  $\sigma_u$  is equal to  $\sigma_c^B$ . Namely, the type I mode is realized. The estimated value of  $e_{max}$  is displayed in Fig. 5. On the other hand, when  $\sigma_c^B < \sigma_c^A$ , which corresponds to the type II mode, then the composite is brittle with a short elongation. The  $\sigma_u$  is then equal to  $\sigma_c^A$ . The transition of the fracture mode occurs at the condition of  $\sigma_c^A = \sigma_c^B$ . In Fig. 5, the vertical line shows this transition.

The maximum pinning force is qualitatively expressed as a function of the inverse grain size 7), 8). However, the quantitative discussion along with the theoretical evalua-

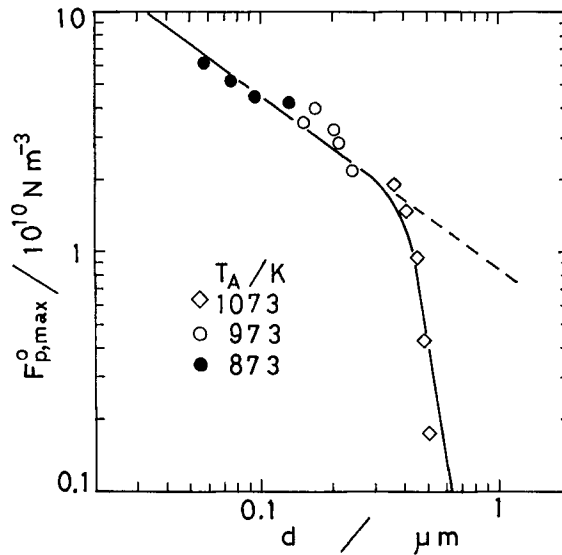


Fig. 7 Grain size dependence of the maximum global pinning force.

tion is rather difficult because it depends strongly on the microstructure 9). In Fig. 7, the pinning force decreases with an increasing grain size. Its dependency can be divided into two parts. The weakly size dependent part is consistent with the data reported by other authors 7), 8), 9) and is proportional to  $d^{-0.71}$ , but not to  $d^{-1}$ . The maximum pinning force is expressed empirically as a function of the grain size by the equation.

$$F_{p,\max}^0 = 0.878d^{-0.71}(1 - \exp(-0.006/d^6)). \quad (13)$$

Now we can reconstruct the critical current  $I_c$  in terms of some representative structure parameters. The total area of the  $Nb_3Sn$  compound layers is given by the equation,

$$S_{Nb_3Sn} = \alpha_b N_f \pi d_f^2 c / d_f (1 - c/d_f), \quad (14)$$

where  $\alpha_b$  is the constant concerning the contribution from the Nb barrier and is 1.073 at present. As  $F_{p,\max}^0$  is expressed by Eq. (13), the critical current near  $B \cong B_{\max}$  is

$$I_c = S_{Nb_3Sn} F_{p,\max}^0 / B. \quad (15)$$

As mentioned in the present text, the layer thickness  $c$  and the grain size  $d$  can be described in terms of annealing time and temperature. Thus the critical current can be

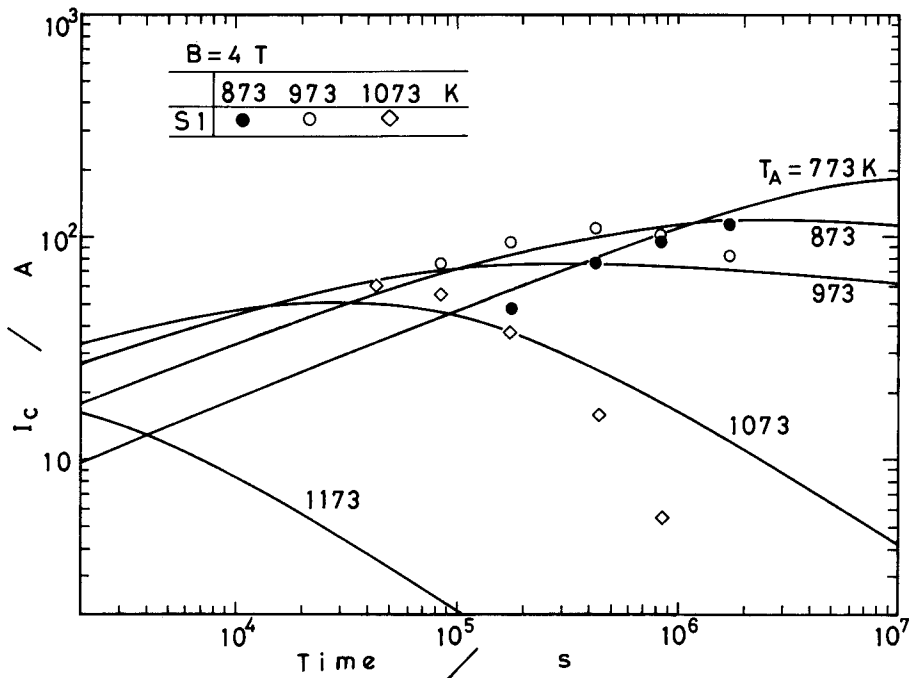


Fig. 8 Critical currents as a function of annealing time for the composite with a filament diameter of 5.3  $\mu\text{m}$ .

assessed at any annealing condition. Fig. 8 shows the annealing time dependence of the critical current at  $B = 4T$ , where the diameter of the Nb filament is  $5.3 \mu\text{m}$ . At a constant temperature,  $I_c$  increases with increasing time at first and reaches a maximum, and then decrease by further annealing. This decrease is attributed to the growth of the grain size of the Nb<sub>3</sub>Sn compound.

#### 4. Conclusion

It is emphasized that the microstructure characterization of multifilamentary composites is important to assess both superconducting and mechanical properties. For the composites with similar shapes, the general description of microstructure is important to design the conductors with optimum performance. The present attempt is concluded to be effective for the purpose.

#### Acknowledgement

The authors express their gratitude to the Ministry of Education, Science and Culture of Japan for the grant-in-aid for energy research(63050044).

#### References

- 1) J. W. Ekin : Superconducting Materials Science-Metallurgy, Fabrication and Applications, ed. by S. Forner and B. B. Schwarz, Plenum Press,(1981), p. 455.
- 2) S. Ochiai, K. Osamura and T. Uehara : J. Mater. Sci., 21(1986)1020.
- 3) S. Ochiai, T. Uehara and K. Osamura : J. Mater. Sci., 21(1986)1027.
- 4) S. Ochiai, K. Osamura and M. Ryoji : Trans. ISIJ, 28(1988)973.
- 5) J. Crank : The Mathematics of Diffusion, Clarendon Press, Oxford, (1956).
- 6) H. Oikawa and A. Hosoi : Scripta Met., 9(1975)823.
- 7) R. M. Scanlan, W. A. Fietz and E. F. Koch : J. Appl. Phys., 46(1975)2244.
- 8) W. Schauer and W. Schelb : IEEE Trans. on Mag., MAG-17(1981)374.
- 9) K. Osamura, S.Ochiai, S. Kondo, M. Namatame and M. Nosaki : J. Mater. Sci., 21(1985)1509.